Received: 24 November 2022 | Accepted: 13 December 2022

DOI: 10.1002/pld3.476

ORIGINAL RESEARCH

A novel CLAVATA1 mutation causes multilocularity in *Brassica rapa*

Hiu Tung Chow | Timmy Kendall | Rebecca A. Mosher

School of Plant Sciences, The University of Arizona, Tucson, Arizona, USA

Correspondence
Rebecca A. Mosher, School of Plant Sciences, The University of Arizona, Tucson, AZ 85721, USA.
Email: rmosher@email.arizona.edu

Funding information
USDA National Institute of Food and Agriculture, Grant/Award Number: ARZT-3039860-G25-578

Abstract

Locules are the seed-bearing structure of fruits. Multiple locules are associated with increased fruit size and seed set, and therefore, control of locule number is an important agronomic trait. Locule number is controlled in part by the CLAVATA-WUSCHEL pathway. Disruption of either the CLAVATA1 receptor-like kinase or its ligand CLAVATA3 can cause larger floral meristems and an increased number of locules. In an EMS mutagenized population of *Brassica rapa*, we identified a mutant allele that raises the number of locules from four to a range of from six to eight. Linkage mapping and genetic analysis support that the mutant phenotype is due to a missense mutation in a *CLAVATA 1* (*CLV1*) homolog. In addition to increased locule number, additional internal gynoecia are formed in *brclv1* individuals, suggesting a failure to terminate floral meristem development, which results in decreased seed production.

KEYWORDS
B. rapa, CLAVATA-WUSCHEL, floral meristem, fruit, gynoecium, locule, seed set

1 | INTRODUCTION

In angiosperm fruit, locules are the chamber surrounding the pericarp that contains the seeds. Locules are derived from the fusion of carpels, the innermost whorls of a flower and the female reproductive structure (Herrera-Ubaldo & de Folter, 2022). During Brassicaceae flower development, carpels fuse into a cylindrical gynoecium separated by thin septa that form locules. Cells in the margins between fused carpels give rise to the ovules, resulting in a row of ovules in each locule. Gynoecia can form from the fusion of two or more carpels, resulting in two or more carpel margins. After fertilization, the gynoecium elongates and differentiates into a silique (the fruit), and the walls of each carpel are known as valves. Generally, the number of valves reflects the number of carpels originally present in a gynoecium, and the number of locules is often equivalent to or slightly fewer than the number of valves.

The early stage of floral development requires the *CLAVATA* (*CLV*) signaling pathway (Somssich et al., 2016). In *A. thaliana* (Arabidopsis), *CLV1* encodes a Leucine-rich repeat (LRR) receptor-like kinase perceiving a small peptide ligand encoded by *CLV3* (Clark et al., 1997; Ogawa et al., 2008). Mutations disrupting *CLV1* cause a range of abnormalities in floral tissues including extra carpels and ectopic floral organs (Clark et al., 1997; Diévart et al., 2003). *clv1* mutants also display a range of silique phenotypes including club-shaped siliques, partial valves/valveless, and extra valves. Mutation of *CLV3* causes multicarpel gynoecia and siliques with extra valves (Fiers et al., 2006; Song et al., 2013). The abnormalities observed in *clv1* and *clv3* mutants are attributed to the disruption of stem cell maintenance, which results in enlarged floral meristems, which results in more cells contributing to carpel development, as well as increased cell division in the valve margins (Durbak & Tax, 2011).

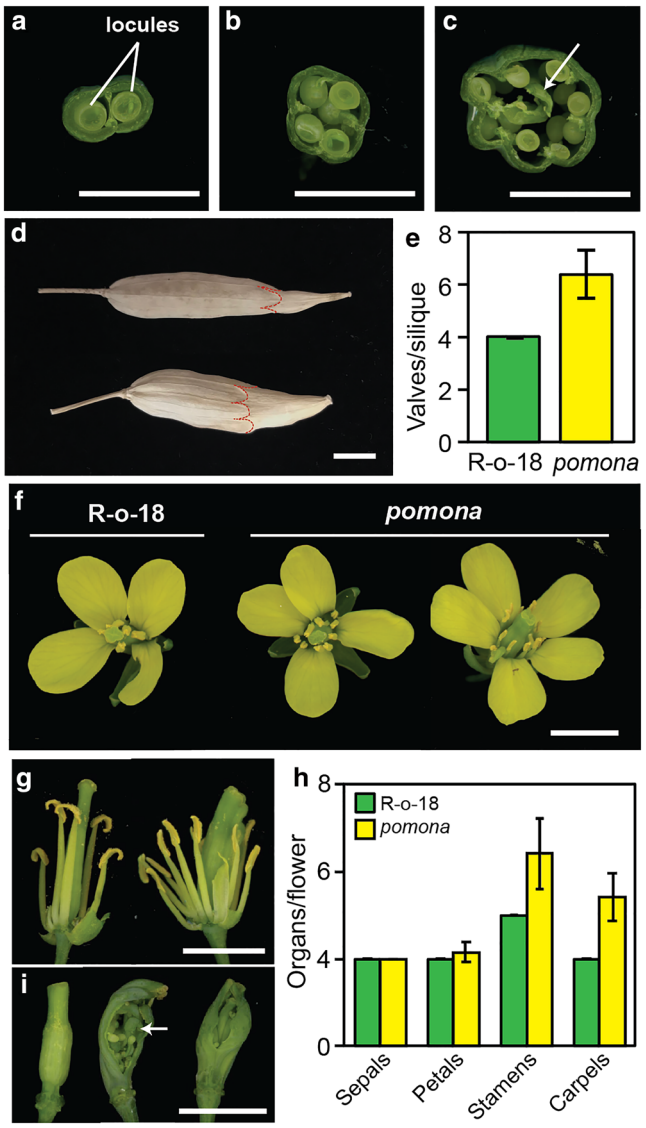

FIGURE 1 *Pomona* displays multilocular phenotype. (a) Simplified floral structure in *Brassica rapa*. (A-C) Cross-section of stage 18 developing siliques from the bilocular variety R500 (a), the tetralocular variety R-o-18 (b), and *pomona* in the R-o-18 background (c). The white arrow points to the ectopic gynoecium growing inside a *pomona* primary gynoecium. Scale bar = .5 cm. (d) Images of complete mature and dried siliques of R-o-18 (top) and *pomona* (bottom) before shattering. The top edges of the valves are marked with dashed red lines. Scale bar = .5 cm. (e) Average number of valves per silique in 180 mature dried siliques from 10 individuals in *pomona* and R-o-18. Error bars represent standard deviation. (f) Represent images of R-o-18 and *pomona* flowers. (g) Enlarged images with petals removed of gynoecia in R-o-18 (left) and *pomona* (right). (h) Average number of floral organs in R-o-18 and *pomona* flowers. Quantification of 150 flowers with enclosed gynoecia as the carpel number in the cracked gynoecia could not be accurately counted. Error bars represent standard deviation. (i) In *pomona* flowers, 84% of the gynoecia were well-enclosed (left), but 16% displayed cracked ovary walls (middle and right), with ectopic gynoecia growing inside (white arrows). Scale bar = .5 cm

Because ovules arise from the carpel margins, ovule/seed number is correlated with carpel/locule number (Herrera-Ubaldo & de Folter, 2022; Xu et al., 2021). The more carpels in the gynoecium, the more cells have the meristematic properties to allow ovule and seed formation. This hypothesis has been tested mostly in the *Brassica* genus, where 2-carpel gynoecia and bilocular siliques are the ancestral state, but some varieties have additional locules. A naturally-occurring single nucleotide polymorphism (SNP) in *B. rapa* (*B. rapa*) *CLV3* (resulting in a Pro-to-Leu substitution at amino acid 76) causes tetralocular siliques and higher seed set (Fan et al., 2014; Yadava et al., 2014). Similarly, multilocularity in a *Brassica juncea* cultivar is controlled by natural variation in two *CLV1* homoeologs (Chen et al., 2018; Xiao et al., 2013, 2018). Induced mutation of the two *CLV3* homologs in *Brassica napus* results in multilocular siliques with higher seed yield and higher 100-seed weight than either single mutant or wild type. However, unlike the natural variants, these induced loss-of-function mutations have additional pleiotropic effects (Yang et al., 2018).

Here we show that a single missense mutation in A07p048430.1_BraROA (*BrCLV1)* increases locule number in *B. rapa*. However, in contrast to the prevailing hypothesis that increasing the number of locules increases seed set, the multilocular fruits of this mutant do not have greater seed production due to additional internal gynoecia that adversely affect seed set. This research provides alternative insights into the engineering of multilocularity to optimize seed yield.

2 | RESULTS

2.1 | Isolation of a novel multilocular mutation in *B. rapa*

Although most varieties of *B. rapa* have the ancestral bilocular character, R-o-18 is tetralocular due to a non-synonymous substitution in *CLV3* (Fan et al., 2014; Katiyar et al., 1998) (Figure 1a,b). In an EMS mutagenized R-o-18 M3 population, we found a mutant that forms additional locules, resulting in siliques that are wider than R-o-18 (Figure 1c,d). We named this mutant *pomona* after the Roman goddess of fruit. Quantifying valve number in dried siliques demonstrated that *pomona* increased valve number from four to six (±.9) (Figure 1e). The developing flowers on *pomona* individuals also had extra petals, anthers, and carpels, with enlarged gynoecia and fasciated stigmas (Figure 1f–h). Cross-sections revealed that ectopic gynoecia began to form inside the primary gynoecium in all individuals. Approximately 16% of flowers displayed more severe abnormalities, including cracked and twisted gynoecia resulted from incompletely fused carpels, and multiple internal gynoecia (Figure 1i). The growth of additional gynoecia suggests that the carpel meristem failed to terminate appropriately, which is commonly seen in *clv* mutants especially *CLV3* alleles (Sablowski, 2007).

To further characterize the mutation, we first crossed *pomona* to R500 (a bilocular *B. rapa* variety). All F1 individuals (n = 10) were bilocular, suggesting that *pomona* is a recessive mutation. Alternatively, the additional valve phenotype of *pomona* might depend on the *CLV3* allele from R-o-18 ($CLV3^{R\text{-}o\text{-}18}$). To test these hypotheses, F1 plants were allowed to self-fertilize, and we conducted a linkage analysis in the F2 population. First, we scored valve number in 331 F2 individuals. The F2 population displayed three phenotypic classes: 221 individuals had two valves, 64 individuals had four valves, and 46 individuals had five to 10 valves (the *pomona* phenotype). We eliminated another 33 individuals for which we were unable to score for valve number due to other developmental defects. These defect might result from additional EMS-derived mutations in the *pomona* background, and might explain the lower-than-expected number of *pomona*-like individuals in the F2 population. Using a derived cleaved amplified polymorphic sequence PCR marker, *CLV3* alleles were identified in the expected Mendelian ratio (11 $CLV3^{R500}$ homozygous, 17 heterozygous, 18 $CLV3^{R\text{-}o\text{-}18}$ homozygous, *p*-value .07) among the *pomona*-like individuals, indicating that the *pomona* phenotype is independent from *CLV3* genotype and is genetically unlinked from *CLV3*.

2.2 | A missense allele of a *CLV1* ortholog is a candidate for *pomona*

To map the mutation, we performed mapping-by-sequencing on a DNA library constructed from pooled DNA of the 46 class III F2 individuals (Table S1). Analysis of the allele frequencies of R-o-18/R500 polymorphisms narrowed the causal region to a ~4.1-Mb interval on chromosome 7 (Figure S1). Further variant analysis revealed seven non-synonymous, EMS-induced SNPs (G-to-A or C-to-T) in coding regions within the interval (Table 1), however only SNPs in *A07p049690.1_BraROA* and *A07p048430.1_BraROA* have 100% of reads supporting the EMS-induced variants (Table 1, highlighted). *A07p049690.1_BraROA* is a putative carboxyphosphoenolpyruvate mutase (BrCPEPM; homologous to *At1g77060*; 86% nucleotide identity, e-value: 3e-163), whereas *A07p048430.1_BraROA* is *BrCLV1* (82% nucleotide identity, e-value: .0). Using domain similarity with AtCLV1 to annotate LRRs and the kinase domain, we determined that the mutation is located at nucleotide 1745 (CDS) within the 20th LRR, causing a serine to asparagine substitution at amino acid 582 (Figure 2a). This is one of two *AtCLV1* homoeologs among the three *B. rapa* subgenomes (Chen et al., 2022). Given the prior knowledge of *clv1* mutant phenotypes, *BrCLV1* is a strong candidate for the gene disrupted in *pomona*.

To further investigate linkage between these two candidate mutations and the multilocular phenotype, we grew an additional 183 F2 individuals and genotyped them for *BrCLV1* and *BrCPEPM* alleles. For the BrCLV1 alleles, we observed 52, 79, and 52 homozygous mutant, heterozygous, and homozygous wild type, respectively. We then phenotyped floral development and observed that the *pomona* phenotype was restricted to homozygous *brclv1* individuals. Forty-nine of 52 *brclv1* homozygotes displayed the *pomona*

TABLE 1 Candidates SNPs in *pomona*

Chr, position	SNP	Gene ID	*A. thaliana*[a]	*B. rapa*[a]	Read depth	Allele Freq.
A07, 23139415	C to T	A07p042720.1	No hits	Nuclear transport factor (predicted)	29	.931
A07, 23219217	C to T	A07p042880.1	At1g69450; early responsive to dehydration protein (ERD4)	CSC1-like protein	17	.9412
A07, 24030963	C to T	A07p043970.1	At1g70520; with unknown function	Cysteine-rich RLK (RECEPTOR-like protein kinase) 2 (CRK2) (predicted)	16	.9375
A07, 25165300	G to A	A07p046680.1	At1g73750, alpha/beta hydropase family protein	Uncharacterized	21	.9524
A07, 25874214	G to A	A07p048430.1	At1g75820; CLAVATA1	CLV1 (predicted)	15	1
A07, 26401682	G to A	A07p049690.1	At1g77060; phosphoenolpyruvate carboxylase family protein	*B. rapa* carboxyvinyl-carboxyphosphonate phosphorylmutase, chloroplastic	34	1
A07, 26703213	C to T	A07p050080.1	No hits	Uncharacterized protein	28	.9286

[a]The hit with the smallest e-value from the BLAST search.

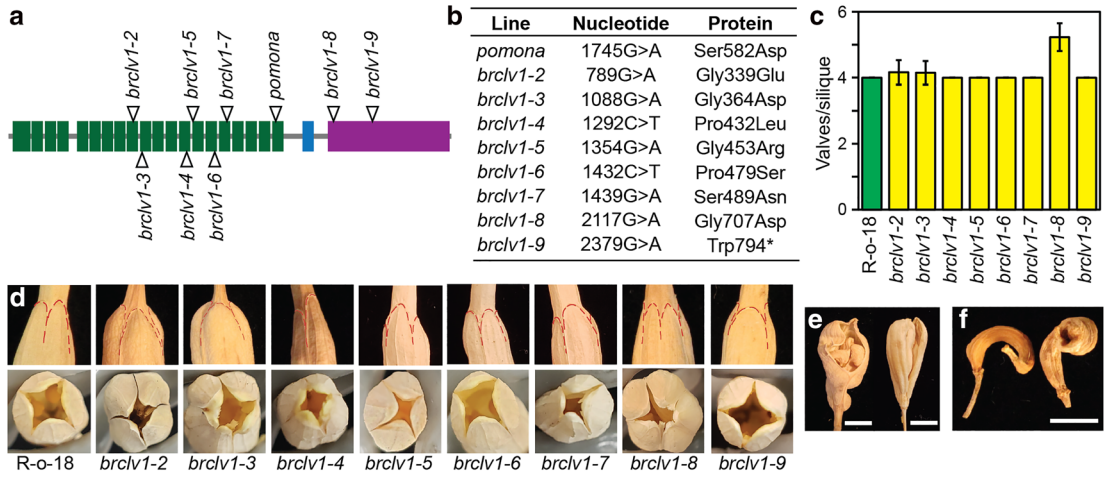

FIGURE 2 TILLING population of *A07p048430.1_BraROA* and allelism test. (a) Scheme of *A07p048430.1_BraROA*. Black, gray, and white rectangles represent LRR, intracellular, and kinase domains, respectively. Asterisk (*) represents the S582N substitution in *pomona*. Triangles indicate the verified point mutation in each allele. (b) Summary of mutation of *pomona* and the TILLING alleles. Line: allele; Nucleotide: position of the point mutation in *A07p048430.1_BraROA* CDS. Protein: position and the substituted amino acid, and Asterisk (*) represents stop codon. (c) Average number of valves per silique were counted in at least 75 siliques per genotype from five individuals. Error bars represent standard deviation. (d) Photos are enlarged portion of siliques. To have better view of valve margins, the first row they are marked with red dashed lines, whereas the bottom row is the aerial look of siliques which beaks were removed. In addition to completely fused siliques showing here for *brclv1-2* and *brclv1-3*, these lines often displayed cracked siliques as shown in Figure 3e. (e) Cracked siliques in *brclv1-2* (left) and *brclv1-3* (right). Scale bar = .5 cm. (f) The F1 of *pomona* x *brclv1-9*. Representative images of the F1

phenotype; the three remaining had more severe developmental phenotypes and failed to produce any siliques. At *BrCPEPM* we identified 49 wild-type, 84 heterozygous, and 50 homozygous individuals. Two of the homozygous *brcpepm* mutants lacked the *pomona* phenotype and four *brcpepm* heterozygotes display the *pomona* phenotype. Taken together, this observation indicates that mutation of *BrCPEPM* is not responsible for the multilocular phenotype, and that the *pomona* mutation is within .3 cM of *BrCLV1*.

2.3 | Additional mutations in BrCLV1 influence silique phenotypes

To functionally validate that a mutation in *BrCLV1* is responsible for the multilocular phenotype, we ordered additional mutations in *A07p048430.1_BraROA* from a sequenced R-o-18 TILLING population (Stephenson et al., 2010) and bred eight mutations to homozygosity. The alleles were renamed from *brclv1-2* to *brclv1-9* (Figure 2a,b). To examine evolutionary conservation at the mutated residues, we aligned BrCLV1 amino acid sequence with CLV1 orthologs in 15 eudicots (Figure S2). With the exception of *brclv1-4* and *brclv1-7*, the amino acids mutated in these alleles are highly conserved. To study the effects of these mutations, we examined the phenotypes of siliques and quantified valve numbers. The *brclv1-8* allele displayed the strongest increase in the number of valve formation with (5.23 ± .42) (Figure 2c,d; Figure S3). Although *brclv1-2* and *brclv1-3* alleles produce just slightly additional valves, these lines displayed shorter beaks (the apical portion of the fruit arising from the style) and club-shaped siliques, and produced additional gynoecia, frequently

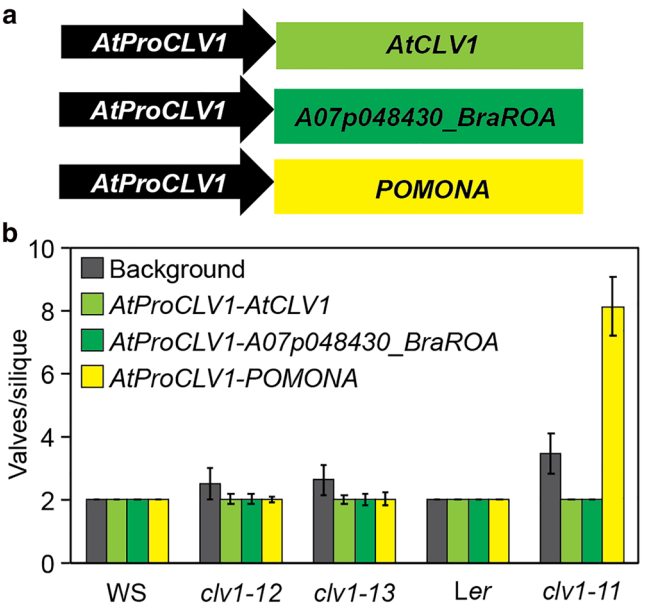

FIGURE 3 *A07p048430.1_BraROA* genetically complements *atclv1*. (a) Schematic diagram of the cloning constructs used for transformation. (b) Average number of valves/silique in each transformants. Fifteen siliques from at least seven lines were counted in each. Columns represent each transformed construct. Error bars represent standard deviation.

resulting in cracked siliques (Figure 2e; Figure S3). The remaining five homozygous mutations (*brclv1-4*, *brclv1-5*, *brclv1-6*, *brclv1-7*, and *brclv1-9*) had no observable effect on silique development or valve number (Figure 2c,d; Figure S3).

Although most of the identified mutations are missense mutants, *brclv1-9* is a nonsense mutation at the catalytic kinase domain which creates a premature stop codon and is expected to result in a loss-of-function allele. We confirmed that neither homozygous nor heterozygous *brclv1-9* plants have any observable silique phenotype. To further confirm that the multilocular phenotype is due to mutation of *A07p048430.1_BraROA*, we crossed *pomona* with *brclv1-9* and examined the F1 progeny. If the *A07p048430.1_BraROA* is not the causal mutation, F1 progeny should be heterozygous for both *pomona* and *BrCLV1* and have wild-type siliques. Although F1 individuals from this cross had siliques with four locules, they shared characteristics with *pomona*, including abnormal siliques and multiple gynoecia. Importantly, none of the F1s from this cross developed healthy siliques (Figure 2f). Because the *pomona x brclv1-9* F1s do not look entirely wild-type, these data suggest that the mutation responsible for multilocularity is allelic to *BrCLV1*.

Because *B. rapa* is not readily transformable, we moved *BrCLV1* transgenes into Arabidopsis *clv1* mutants (Figure 3a). We chose *clv1-11*, *clv1-12*, and *clv1-13* as they are null mutants with increased number of carpels/valves (Diévart et al., 2003), and we used both the wild-type and *pomona* alleles of *BrCLV1*. We also transformed the wild-type *AtCLV1* driven by the same promoter in parallel as a control. Both *AtCLV1* and *BrCLV1* wild-type transgenes complemented the mutant phenotype in *clv1-11*, *clv1-12*, and *clv1-13*, confirming that the transgenes were correctly expressed (Figure 3b). The transgene carrying the *pomona* allele complemented the mutant phenotype of *clv1-12* and *clv1-13*, both of which are in the WS background, but enhanced the mutant phenotype of *clv1-11*, which is in the Landsberg *erecta* (*Ler*) background (Figure 3b). This finding is consistent with a previous observation that ecotype background modifies the *clv1* phenotype (Diévart et al., 2003; Durbak & Tax, 2011). Our experimental findings collectively support that the missense mutation in *BrCLV1* is the causal mutation leading to multilocularity in *B. rapa*. Hereby, *pomona* was renamed as *brclv1-1*.

2.4 | Seed yield in *brclv1-1*

The *brclv1-1* allele described here was initially identified from an M3 EMS-mutagenized population based on partial seed yield restoration in the *nrpd1a-2* background (Grover et al., 2018). In the mapping data, there was no significant change of allele frequency around *NRPD1a* (*A09p015000.1_BraROA*) on chromosome 9. *NRPD1a* also segregated as expected in the F2 mapping population, confirming that the multilocularity phenotype is independent of *NRPD1a*. Because *brclv1-1 nrpd1a-2* has higher seed yield than *nrpd1a-2* (Figure S4), we asked

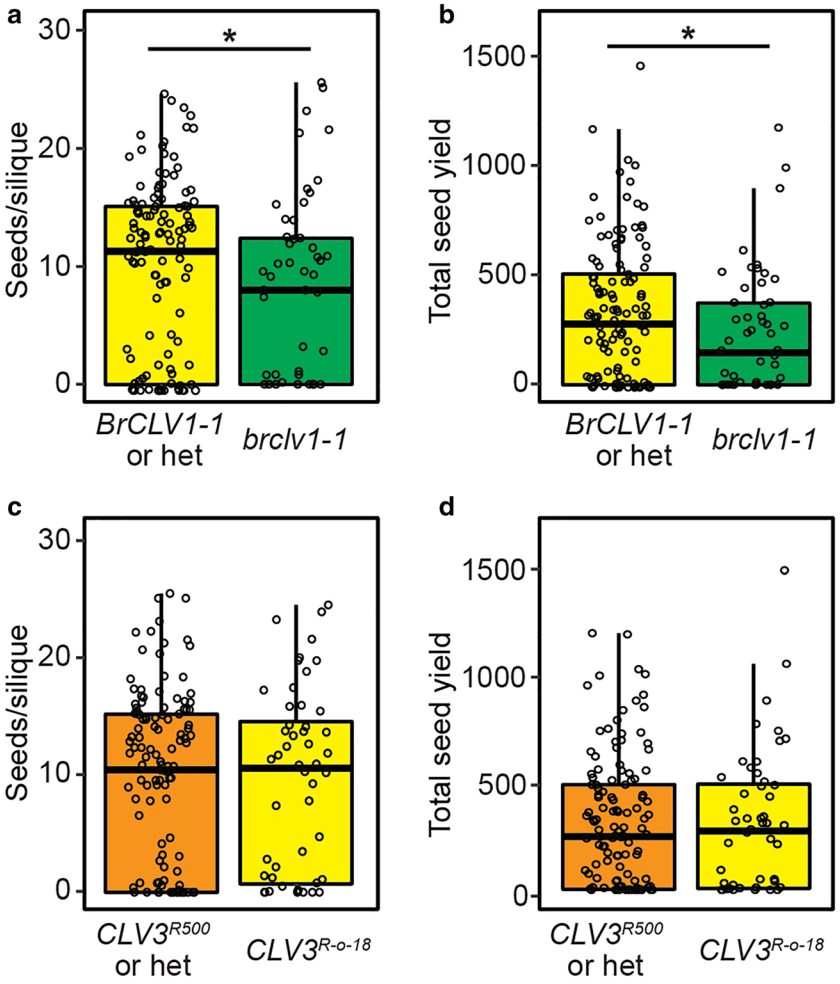

FIGURE 4 Br*CLV1* and Br*CLV3* have subtle effects in boosting seed yield. (a, b) Seed yield in Br*CLV1* alleles from the segregating F2 population. Boxplots of seeds/silique number per plant (a) and total seed yield per plant (b). Asterisk above denotes significant difference according to two-sample *t*-test (*p*-value of (a) .017 < .05; (b) .020 < .05). (c, d) Similar analysis as above but for *CLV3* alleles. No significant difference between comparing groups according to two-sample *t*-test.

whether *brclv1-1* alone caused higher seed set. Because *NRPD1a* is required for seed development, we eliminated homozygous *nrpd1a-2* individuals in the following analyses. We then compared seed production between wild-type, heterozygous, and homozygous *brclv1-1* individuals from the F2 population. In contrast to the *nrpd1a-2* background, both seeds per silique and total seed counts demonstrate that fewer seeds were produced in *brclv1-1* homozygotes (Figure 4a,b). Because these individuals are from the mapping population, they are also segregating for the $CLV3^{R\text{-}o\text{-}18}$ allele, which is associated with higher seed production (Fan et al., 2014). To determine the extent to which the $CLV3^{R\text{-}o\text{-}18}$ allele modified the yield parameters in our population, we measure seeds per silique and total seed count for all *CLV3* allelic combinations. Surprisingly, $CLV3^{R\text{-}o\text{-}18/R\text{-}o\text{-}18}$ has only subtle effects on both seed parameters in this population under these conditions (Figure 4c,d). Because *CLV1* and *CLV3* are in the same pathway, we further asked if *BrCLV1* acted additively with $CLV3^{R\text{-}o\text{-}18}$ in controlling seed set. We tested the effect of *BrCLV1-1* alleles within the $CLV3^{R\text{-}o\text{-}18/R\text{-}o\text{-}18}$ population. The sample size of this experiment was relatively small because three unlinked mutated genes were considered. In this case, there was a slight reduction (p-value < .05, two-sample t-test) on seed yield in individuals carrying *brclv1-1/brclv1-1* (Figure S5).

3 | DISCUSSION

An increased number of floral organs, including the carpels that develop into the locules of the fruit, can be attributed to excess accumulation of stem cells in the floral meristem or mutation of floral homeotic genes (Denay et al., 2017; Shang et al., 2019). CLV1 is involved in regulating stem cell proliferation in the shoot apical meristem (SAM). *CLV1* mutation causes an enlarged SAM and therefore more stem cells for floral meristem (FM) development, eventually causing an increased number of floral organs. Here, we demonstrate that *pomona*, a missense mutation in the *BrCLV1* LRR domain, causes increased floral organs, resulting in multilocular fruits.

The *pomona* mutation is recessive, as heterozygotes are indistinguishable from wild type. However, when a *pomona* allele is in *trans* with a presumed loss-of-function allele (*brclv1-9*), the resulting plants do not completely phenocopy *pomona* homozygotes, suggesting that dosage of the mutant protein might influence phenotype in the absence of wild-type protein. Similar complexities are observed when the mutant *pomona* allele is introduced into multiple *atclv1* null backgrounds. *Brclv1-1* causes multilocularity in Arabidopsis only in the *clv1-11* background. This observation suggests that the phenotype of *brclv1-1* mutation has ecotype-specific effects, perhaps due to the *erecta* mutation in this genetic background (Diévart et al., 2003; Durbak & Tax, 2011). ERECTA is a LRR-receptor like kinase acting in a pathway parallel to CLV1 to confine *WUS* expression during floral meristem development (Mandel et al., 2014). Recent biochemical and genetic analysis suggests that ERECTA also serves as an upstream regulator of CLV3 in controlling shoot apical meristem maintenance (Zhang et al., 2021). The enhanced phenotype observed when *brclv1-1* is expressed in *clv1-11* could be due to additive ectopic WUS induction by Ler-*ERECTA* and *brclv1*, resulting more carpels/valves formation. Our results highlight the many different phenotypes that can arise due to variation in *CLV1*.

Although multilocularity is associated with increased seed set in Brassica species, we do not detect increased seed production among the *brclv1-1* individuals tested here. One possibility is that the genetic load in these lines due to other EMS mutations could adversely reduce seed production. Such mutations might explain the wide deviation in seed production values for *BrCLV1* individuals, including many individuals that did not produce seeds (Figure 4a). However, we also observed that *brclv1-1* multilocular siliques consistently contained additional internal gynoecia, which occupied cavity space where the ovule/seeds should develop. These internal gynoecia, which also sometimes prevented fusion of the primary carpels, likely arose through failure to terminate stem cell activity. *CLV1* transcripts are repressed by KNUCKLES (KNU) during early floral development, resulting in termination of stem cell activity, which necessary for FM determinacy (Shang et al., 2021; Sun et al., 2009, 2019). Although the KNU pathway is not well-characterized in *B. rapa*, in Arabidopsis, KNU binds to both the promoter and first exon, a region close to the *pomona* mutation (Shang et al., 2021), suggesting that KNU regulation might be disrupted in *brclv1-1*.

Although additional internal gynoecia and secondary EMS mutations likely underlie the reduced seed set of *brclv1-1* fruits, *brclv1-1* was originally discovered in a suppressor screen looking for increased seed production in the *nrpd1* background, indicating that *brclv1* influences seed development in some genetic contexts. The additional gynoecia occupy internal space of ovary which constraints seed set, but such restriction might be eased in the *nrpd1* mutant, which has many small aborted seeds. In addition to its well-known role in stem cell maintenance, CLV1 also localizes to plasmodesmata in the root and is hypothesized to regulate the movement of developmental factors there (Stahl et al., 2013; Stahl & Simon, 2013). Intercellular movement of siRNAs produced by NRPD1 is hypothesized to influence plant reproduction (Grover et al., 2020; Long et al., 2021), and it is also possible that the CLV1 and NRPD1 pathways intersect via siRNA movement.

The *brclv1-1* is an allele causing multilocular fruit production. Its potential of inducing seed yield could be maximized if the second site suppressor which reduces the internal gynoecia was found. Given the strong phenotype, it also provides fascinating molecular and genetic resources for resolving how CLV1 is involved in carpel development and regulation.

4 | MATERIALS AND METHODS

4.1 | Plant materials and growth conditions

All plants were grown in a greenhouse (*B. rapa*) or growth chamber (*Arabidopsis*) at 18° C with 16 h light. Unless mentioned otherwise, all *B. rapa* plants used throughout the study are in R-o-18, an inbred line

of the *B. rapa* subsp. trilocularis (Rana et al., 2004; Rusholme et al., 2007). *clv11-11*, *clv1-12*, and *clv1-13* are null *clv1* mutant characterized before (Diévart et al., 2003). *clv1-12* and *clv1-13* were obtained from ABRC. *clv1-11* was a gift from Professor Zachary Nimchuk.

4.2 | Ethyl methanesulfonate (EMS) mutagenesis and isolation of *pomona*

EMS treatment of *nrpd1a-2* seed was performed as described in Stephenson et al., 2010. Briefly, *nrpd1a-2* seeds (four to six generations backcrossed from the original TILLING mutation) were treated with .2% EMS for 16 h, followed by multiple washing with .02% Tween20. The treated M1 seeds were grown and selfed seed were collected. Pools of M2 seed were propagated and M2 individuals with increased seed production were selected. *Brclv1* was recovered in this M2 generation and characterized in multiple M3 individuals.

4.3 | Map-based cloning of multilocular phenotype

M3 *brclv1* flowers were emasculated 1 day prior to anthesis, and then were pollinated with R500 pollen. The resulting F1 individuals were self-pollinated to generate an F2 population. F2 individuals from a single F1 parent were sown and phenotyped for locule number.

DNA was extracted from 46 multilocular F2 individuals using GeneJET Plant Genomic DNA Purification kit (Thermo Scientific). After quantification by Nanodrop, equal amounts of DNA were pooled and 2 μg of pooled DNA in 100 μl was fragmented by Bioruptor Pico (30 s ON/90 s OFF, three cycles, centrifuge 10 s; repeat one time). Forty microliters of the fragmented DNA was used for library construction with a NEXTflex PCR-Free DNA-Seq Kit (Bioo Scientific) according to the manufacturer instructions. Barcoded libraries were quantified using a Bioanalyzer (Agilent Technologies), and paired-end sequenced on an Illumina NextSeq 500 at The University of Arizona Genetics Core.

4.4 | Sequencing read and variant analyses

Trimmed reads were first aligned to the *B. rapa* R500 genome (version 1.2; Greenham et al., 2020) using Bowtie v2.2.4 (Langmead & Salzberg, 2012) and SNPs were used to identify linkage with the causal mutation. Variant calling was conducted by bcftools mpileup and only SNPs with quality score ≥30 and read depth >10 were retained. bcftools query was used to extract information of each variant call and the results were further parsed using R to compute allele frequencies. For markers ≥50.0 map units from the causal mutation, the allele frequencies were expected to be ∼.5; whereas markers linked to the mutation have higher allele frequencies. This analysis demonstrated linkage to the lower arm of chromosome 7.

To identify EMS-induced mutations in this region, read alignment and variant calling were conducted as described above but using the *B. rapa* R-o-18 genome (version 2.3). Only G-to-A and C-to-T, and mutant allele frequency >.9 SNPs within the mapping interval were retained for further analysis. To predict the effects of mutations, SnpRff was used to annotate the variants and predict their effects on genes (Cingolani et al., 2012).

4.5 | Genotyping *BrCLV3*, *BrCLV1*, and *BrCPEPM*

Genotyping primers were designed by dCAPS Finder 2.0 http://helix.wustl.edu/dcaps/ (Neff et al., 2002). The R-o-18 and R500 alleles at *BrCLV3* were genotyped with GATCGGAATCGGGAAGATGACAA and CGACGCTGATGAGGATCAACGC and digested with *HindIII*. *brclv1-1* was genotyped with GATCGGAATCGGGAAGATGACAA and CGACGCTGATGAGGATCAACGC and digested with *AluI*. Additional alleles at *BrCLV1* from the RevGen UK TILLING population (Stephenson et al., 2010) were verified through amplifying and sequencing regions of *BrCLV1* (forward1: AAACATCCCACCAGAACTCTCC and reverse1: GGAGATTAAGGAAGTGCAGCGAGA or forward2: gCTAACAATTGGTTTACCGGTTTAAGC and reverse2: GCTATCGAAGACATACACTCAGAAGCA). *BrCPEPM* was genotyped with GCACAAAGGGTTTCAGAGTCTGC and CTCCAAGTGACCTCTCGTGGATC and digested with *BamHI*.

4.6 | Cloning constructs and transformation

All cloning constructs were based on a pGGZ003 vector containing a UBQ10 promoter and a UBQ terminator (Lampropoulos et al., 2013). To remove the existing coding sequence between the promoter and terminator, the vector was digested with *NotI* and *BamHI* and gel purified. Gibson assembly modules were created via PCR amplification from genomic DNA of a 4005-bp *AtProCLV1* and approximately 3.3 kb sequences from *AtCLV1*, *BrCLV1*, or *brclv1-1* using primers in Table S2. The modules were joined to the backbone through a Gibson assembly reaction at 50°C for 1.5 h and immediately transformed into *E. coli*. Sequences were confirmed by enzyme digestion and sequencing before transformation into chemically competent *Agrobacterium tumefaciens* GV3101 carrying the pSOUP helper plasmid for transformation of Arabidopsis by floral dip (Clough & Bent, 1998). T1 seeds were selected based on Basta resistance, and T2 plants from lines with a single insertion site were used for phenotyping.

4.7 | Yield assessment

The number of seeds per silique were counted from siliques collected from the main stem. The total number of seeds was assayed from all seeds collected from the whole plant.

4.8 | Evolutionary comparison

The genomic sequence of genes in the mapping interval were used as query sequences to search against the Arabidopsis (TAIR 10) genome using BLAST. The best hit with e-value lower than 1e-10 was reported. Retention of homologous copies among three subgenomes of *B. rapa* was retrieved from the BRAD database (http://brassicadb.cn/).

CLV1 orthologs in other species were obtained from Phytozome v13 (https://phytozome-next.jgi.doe.gov) (Goodstein et al., 2012) with following PAC gene identifiers: *C. rubella*, 20904558; *C. sativa*, 16979492, *E. salsugineum*, 20191806; *C. papaya*, 16415260; *Camellia sinensis*, 18092691; *R. communis*, 16822209: *C. esculenta*, 32335358; *M. truncatula*, 31112997; *F. vesca*, 27262373; *P. persica*, 32118556; *E. grandis*, 32053920; *A. hypochondriacus*, 32828513; *A. coerulea*, 33062625; and *S. polyrhiza*, 31521071.

ACKNOWLEDGMENTS

This work is supported by project number ARZT-3039860-G25-578 from the USDA National Institute of Food and Agriculture to RAM. We are grateful to Keign Vedvick for assistance with the EMS mutant screens, and to Renee Grambihler, Collin Eckhauser, and Jeff Clark for assisting with phenotyping and seed counting. Thanks also go to Dr. Frans Tax for reviewing the manuscript, to Dr. Michael Ottman for use of his seed counter, and to Dr. Zachary Nimchuk for the *atclv1-11 line*. DNA sequencing was conducted by the University of Arizona Genetics Core.

CONFLICT OF INTEREST

The Authors did not report any conflict of interest.

AUTHOR CONTRIBUTIONS

Hiu Tung Chow: Investigation, Formal analysis, Visualization, Writing - Original Draft, Writing - Review & Editing. **Timmy Kendall:** Investigation. **Rebecca Mosher:** Conceptualization, Methodology, Visualization, Writing - Review & Editing, Project Administration.

DATA AVAILABILITY STATEMENT

Sequence data from this study reside in the NCBI SRA under accession number PRJNA882476.

ORCID

Hiu Tung Chow https://orcid.org/0000-0003-0493-6546
Rebecca A. Mosher https://orcid.org/0000-0003-2195-0825

REFERENCES

Chen, C., Xiao, L., Li, X., & Du, D. (2018). Comparative mapping combined with map-based cloning of the Brassica juncea genome reveals a candidate gene for multilocular rapeseed. *Frontiers in Plant Science*, *9*, 1744. https://doi.org/10.3389/fpls.2018.01744

Chen, H., Wang, T., He, X., Cai, X., Lin, R., Liang, J., Wu, J., King, G., & Wang, X. (2022). BRAD V3.0: An upgraded Brassicaceae database. *Nucleic Acids Research*, *50*, D1432–D1441. https://doi.org/10.1093/nar/gkab1057

Cingolani, P., Platts, A., Wang, L. L., Coon, M., Nguyen, T., Wang, L., Land, S. J., Lu, X., & Ruden, D. M. (2012). A program for annotating and predicting the effects of single nucleotide polymorphisms, SnpEff: SNPs in the genome of Drosophila melanogaster strain w1118; iso-2; iso-3. *Fly (Austin)*, *6*, 80–92. https://doi.org/10.4161/fly.19695

Clark, S. E., Williams, R. W., & Meyerowitz, E. M. (1997). The CLAVATA1 gene encodes a putative receptor kinase that controls shoot and floral meristem size in Arabidopsis. *Cell*, *89*, 575–585. https://doi.org/10.1016/S0092-8674(00)80239-1

Clough, S. J., & Bent, A. F. (1998). Floral dip: A simplified method forAgrobacterium-mediated transformation ofArabidopsis thaliana. *The Plant Journal*, *16*, 735–743. https://doi.org/10.1046/j.1365-313x.1998.00343.x

Denay, G., Chahtane, H., Tichtinsky, G., & Parcy, F. (2017). A flower is born: An update on Arabidopsis floral meristem formation. *Current Opinion in Plant Biology*, *35*, 15–22. https://doi.org/10.1016/j.pbi.2016.09.003

Diévart, A., Dalal, M., Tax, F. E., Lacey, A. D., Huttly, A., Li, J., & Clark, S. E. (2003). CLAVATA1 dominant-negative alleles reveal functional overlap between multiple receptor kinases that regulate meristem and organ development. *Plant Cell*, *15*, 1198–1211. https://doi.org/10.1105/tpc.010504

Durbak, A. R., & Tax, F. E. (2011). CLAVATA signaling pathway receptors of Arabidopsis regulate cell proliferation in fruit organ formation as well as in meristems. *Genetics*, *189*, 177–194. https://doi.org/10.1534/genetics.111.130930

Fan, C., Wu, Y., Yang, Q., Yang, Y., Meng, Q., Zhang, K., Li, J., Wang, J., & Zhou, Y. (2014). A novel single-nucleotide mutation in a CLAVATA3 gene homolog controls a multilocular silique trait in Brassica rapa L. *Molecular Plant*, *7*, 1788–1792. https://doi.org/10.1093/mp/ssu090

Fiers, M., Golemiec, E., van der Schors, R., van der Geest, L., Li, K. W., Stiekema, W. J., & Liu, C.-M. (2006). The CLAVATA3/ESR motif of CLAVATA3 is functionally independent from the nonconserved flanking sequences. *Plant Physiology*, *141*, 1284–1292. https://doi.org/10.1104/pp.106.080671

Goodstein, D. M., Shu, S., Howson, R., Neupane, R., Hayes, R. D., Fazo, J., Mitros, T., Dirks, W., Hellsten, U., Putnam, N., & Rokhsar, D. S. (2012). Phytozome: A comparative platform for green plant genomics. *Nucleic Acids Research*, *40*, D1178–D1186. https://doi.org/10.1093/nar/gkr944

Greenham, K., Sartor, R. C., Zorich, S., Lou, P., Mockler, T. C., & McClung, C. R. (2020). Expansion of the circadian transcriptome in Brassica rapa and genome-wide diversification of paralog expression patterns. *Elife*, *9*, e58993. https://doi.org/10.7554/eLife.58993

Grover, J. W., Burgess, D., Kendall, T., Baten, A., Pokhrel, S., King, G. J., Meyers, B. C., Freeling, M., & Mosher, R. A. (2020). Abundant expression of maternal siRNAs is a conserved feature of seed development. *Proceedings of the National Academy of Sciences of the United States of America*, *117*, 15305–15315. https://doi.org/10.1073/pnas.2001332117

Grover, J. W., Kendall, T., Baten, A., Burgess, D., Freeling, M., King, G. J., & Mosher, R. A. (2018). Maternal components of RNA-directed DNA methylation are required for seed development in Brassica rapa. *The Plant Journal*, *94*, 575–582. https://doi.org/10.1111/tpj.13910

Herrera-Ubaldo, H., & de Folter, S. (2022). Gynoecium and fruit development in Arabidopsis. *Development*, *149*(5), dev200120. https://doi.org/10.1242/dev.200120

Katiyar, R. K., Chamola, R., & Chopra, V. L. (1998). Tetralocular mustard, Brassica juncea: New promising variability through interspecific hybridization. *Plant Breeding*, *117*, 398–399. https://doi.org/10.1111/j.1439-0523.1998.tb01962.x

Lampropoulos, A., Sutikovic, Z., Wenzl, C., Maegele, I., Lohmann, J. U., & Forner, J. (2013). GreenGate - a novel, versatile, and efficient cloning

system for plant Transgenesis. *PLoS ONE*, *8*, e83043. https://doi.org/10.1371/journal.pone.0083043

Langmead, B., & Salzberg, S. L. (2012). Fast gapped-read alignment with bowtie 2. *Nature Methods*, *9*, 357–359. https://doi.org/10.1038/nmeth.1923

Long, J., Walker, J., She, W., Aldridge, B., Gao, H., Deans, S., Vickers, M., & Feng, X. (2021). Nurse cell-–derived small RNAs define paternal epigenetic inheritance inArabidopsis. *Science*, *373*, eabh0556. https://doi.org/10.1126/science.abh0556

Mandel, T., Moreau, F., Kutsher, Y., Fletcher, J. C., Carles, C. C., & Williams, L. E. (2014). The ERECTA receptor kinase regulates Arabidopsis shoot apical meristem size, phyllotaxy and floral meristem identity. *Development*, *141*, 830–841. https://doi.org/10.1242/dev.104687

Neff, M. M., Turk, E., & Kalishman, M. (2002). Web-based primer design for single nucleotide polymorphism analysis. *TRENDS in Genetics*, *18*(12), 613–615. https://doi.org/10.1016/S0168-9525(02)02820-2

Ogawa, M., Shinohara, H., Sakagami, Y., & Matsubayashi, Y. (2008). Arabidopsis CLV3 peptide directly binds CLV1 ectodomain. *Science*, *319*, 294. https://doi.org/10.1126/science.1150083

Rana, D., van den Boogaart, T., O'Neill, C. M., Hynes, L., Bent, E., Macpherson, L., Park, J. Y., Lim, Y. P., & Bancroft, I. (2004). Conservation of the microstructure of genome segments in Brassica napus and its diploid relatives. *The Plant Journal*, *40*, 725–733. https://doi.org/10.1111/j.1365-313X.2004.02244.x

Rusholme, R. L., Higgins, E. E., Walsh, J. A., & Lydiate, D. J. (2007). Genetic control of broad-spectrum resistance to turnip mosaic virus in Brassica rapa (Chinese cabbage). *The Journal of General Virology*, *88*, 3177–3186. https://doi.org/10.1099/vir.0.83194-0

Sablowski, R. (2007). Flowering and determinacy in Arabidopsis. *Journal of Experimental Botany*, *58*, 899–907. Available at: [Accessed July 21, 2022]. https://doi.org/10.1093/jxb/erm002

Shang, E., Ito, T., & Sun, B. (2019). Control of floral stem cell activity in Arabidopsis. *Plant Signaling & Behavior*, *14*. https://doi.org/10.1080/15592324.2019.1659706

Shang, E., Wang, X., Li, T., Guo, F., Ito, T., & Sun, B. (2021). Robust control of floral meristem determinacy by position-specific multifunctions of KNUCKLES. *Proceedings of the National Academy of Sciences of the United States of America*, *118*, e2102826118. https://doi.org/10.1073/pnas.2102826118

Somssich, M., Je, B. I., Simon, R., & Jackson, D. (2016). CLAVATA-WUSCHEL signaling in the shoot meristem. *Development*, *143*, 3238–3248. https://doi.org/10.1242/dev.133645

Song, X.-F., Guo, P., Ren, S.-C., Xu, T.-T., & Liu, C.-M. (2013). Antagonistic peptide technology for functional dissection of CLV3/ESR genes in Arabidopsis. *Plant Physiology*, *161*, 1076–1085. https://doi.org/10.1104/pp.112.211029

Stahl, Y., Grabowski, S., Bleckmann, A., Kühnemuth, R., Weidtkamp-Peters, S., Pinto, K. G., Kirschner, G. K., Schmid, J. B., Wink, R. H., Hülsewede, A., Felekyan, S., Seidel, C. A. M., & Simon, R. (2013). Moderation of Arabidopsis root stemness by CLAVATA1 and ARABIDOPSIS CRINKLY4 receptor kinase complexes. *Current Biology*, *23*, 362–371. https://doi.org/10.1016/j.cub.2013.01.045

Stahl, Y., & Simon, R. (2013). Gated communities: Apoplastic and symplastic signals converge at plasmodesmata to control cell fates. *Journal of Experimental Botany*, *64*, 5237–5241. https://doi.org/10.1093/jxb/ert245

Stephenson, P., Baker, D., Girin, T., Perez, A., Amoah, S., King, G. J., & Østergaard, L. (2010). A rich TILLING resource for studying gene function in Brassica rapa. *BMC Plant Biology*, *10*, 62. https://doi.org/10.1186/1471-2229-10-62

Sun, B., Xu, Y., Ng, K.-H., & Ito, T. (2009). A timing mechanism for stem cell maintenance and differentiation in the Arabidopsis floral meristem. *Genes & Development*, *23*, 1791–1804. https://doi.org/10.1101/gad.1800409

Sun, B., Zhou, Y., Cai, J., Shang, E., Yamaguchi, N., Xiao, J., Looi, L. S., Wee, W. Y., Gao, X., Wagner, D., & Ito, T. (2019). Integration of transcriptional repression and polycomb-mediated silencing of WUSCHEL in floral meristems. *Plant Cell*, *31*, 1488–1505. https://doi.org/10.1105/tpc.18.00450

Xiao, L., Li, X., Liu, F., Zhao, Z., Xu, L., Chen, C., Wang, Y., Shang, G., & Du, D. (2018). Mutations in the CDS and promoter of BjuA07.CLV1 cause a multilocular trait in Brassica juncea. *Scientific Reports*, *8*, 5339. https://doi.org/10.1038/s41598-018-23636-4

Xiao, L., Zhao, H., Zhao, Z., du, D., Xu, L., Yao, Y., Zhao, Z., Xing, X., Shang, G., & Zhao, H. (2013). Genetic and physical fine mapping of a multilocular gene Bjln1 in Brassica juncea to a 208-kb region. *Molecular Breeding*, *32*, 373–383. https://doi.org/10.1007/s11032-013-9877-1

Xu, P., Wang, X., Dai, S., Cui, X., Cao, X., Liu, Z., & Shen, J. (2021). The multilocular trait of rapeseed is ideal for high-yield breeding. *Plant Breeding*, *140*, 65–73. https://doi.org/10.1111/pbr.12880

Yadava, S. K., Paritosh, K., Panjabi-Massand, P., Gupta, V., Chandra, A., Sodhi, Y. S., Pradhan, A. K., & Pental, D. (2014). Tetralocular ovary and high silique width in yellow sarson lines of Brassica rapa (subspecies trilocularis) are due to a mutation in Bra034340 gene, a homologue of CLAVATA3 in Arabidopsis. *Züchter Genetics and Breeding Research*, *127*, 2359–2369. https://doi.org/10.1007/s00122-014-2382-z

Yang, Y., Zhu, K., Li, H., Han, S., Meng, Q., Khan, S. U., Fan, C., Xie, K., & Zhou, Y. (2018). Precise editing of CLAVATA genes in Brassica napus L. regulates multilocular silique development. *Plant Biotechnology Journal*, *16*, 1322–1335. https://doi.org/10.1111/pbi.12872

Zhang, L., DeGennaro, D., Lin, G., Chai, J., & Shpak, E. D. (2021). ERECTA family signaling constrains CLAVATA3 and WUSCHEL to the center of the shoot apical meristem. *Development*, *148*, dev189753. https://doi.org/10.1242/dev.189753

SUPPORTING INFORMATION

Additional supporting information can be found online in the Supporting Information section at the end of this article.

How to cite this article: Chow, H. T., Kendall, T., & Mosher, R. A. (2023). A novel CLAVATA1 mutation causes multilocularity in *Brassica rapa*. *Plant Direct*, *7*(1), e476. https://doi.org/10.1002/pld3.476